

The disc-jet coupling in Aql X-1*

Valeriu Tudose[†]

Astronomical Institute, University of Amsterdam

E-mail: v.m.tudose@uva.nl

Rob Fender

School of Physics and Astronomy, University of Southampton

E-mail: r.fender@soton.ac.uk

Manuel Linares

Astronomical Institute, University of Amsterdam

E-mail: linares@uva.nl

Dipankar Maitra

Astronomical Institute, University of Amsterdam

E-mail: d.maitra@uva.nl

We present a multiwavelength analysis of the outbursts from the neutron star X-ray binary Aql X-1. We focus on three outbursts for which quasi-simultaneous data in radio, optical and X-ray bands exist. We find evidence that the disc/jet coupling in Aql X-1 is similar to the one documented for black hole X-ray binaries, at least from the point of view of the general behaviour revealed during outbursts.

VII Microquasar Workshop: Microquasars and Beyond

September 1 - 5, 2008

Foca, Izmir, Turkey

*An extended version of the paper to be submitted to MNRAS.

[†]Speaker.

1. Introduction

The low-mass X-ray binary (LMXRB) Aquila X-1 (Aql X-1) is a recurrent soft X-ray transient which shows quasi-periodic outbursts about once a year (e.g. [40]). The compact object in the system is a neutron star as implied by the detection of type I X-ray bursts (e.g. [23]). The companion is a main sequence star likely of the spectral type K7 [7]. The properties of Aql X-1 place it in the class of atoll sources [33] and recent observations of coherent pulsations in the persistent X-ray emission [5] makes it the ninth accretion-powered millisecond X-ray pulsar (AMP) known to date. The system also exhibits X-ray burst oscillations (e.g. [38]) and kHz quasi-periodic oscillations (QPOs), both lower kHz QPO (e.g. [11]), and upper kHz QPO (a single detection, [1]).

The optical counterpart has in quiescence a V band magnitude of 21.60 and is only 0.48 arc-sec away from a contaminating star of V band magnitude 19.42 [7] thus complicating the optical studies.

Besides the orbital period close to 19 h (e.g. [6, 43]), little is known about the other parameters of the system. The inclination of the orbit is poorly constrained, with values ranging between 36 degree and 70 degree [39, 18, 43]. The distance to Aql X-1 is not exactly known, but different estimates place it in the range 4–6.5 kpc [7, 37, 21].

Reports of radio observations of Aql X-1 are extremely scarce in the literature: [35, 36]. This is not surprising since the atoll sources are quite difficult to observe given their sub-mJy flux density levels at cm wavelengths even during outbursts [13]. Basically, although they represent the bulk of the XRBs population [15], only a handful of atoll sources have been detected in radio (e.g. [20, 27, 28, 29, 31]). The atolls show two main X-ray states [19, 41], identifiable in the colour-colour diagrams (CDs): a softer, “banana state” (BS), and a harder, “island state” (IS). In order to accommodate observations with harder X-ray spectrum, at low count rates, a new state was introduced (e.g. [32]): “extreme island state” (EIS). From the point of view of the X-ray spectral and timing properties, atoll sources (especially in the EIS) share many similar properties with the black hole XRBs (BHXRBS) in the low-hard state (e.g. [42]). In the case of 4U 1728-34 a correlation was found between the radio and X-ray fluxes in the IS [28, 30], resembling the relation established for BHXRBS in the low-hard state ([9, 16, 17, 10], but see also [44]).

2. Observations

2.1 Radio

We have analyzed all the public Very Large Array (VLA) radio data between 1986 February and 2005 December containing observations of Aql X-1 (close to 100 epochs). The majority of the observations were carried out in the multi-frequency mode, particularly at 4.9 and 8.4 GHz. Other frequencies, namely 1.5 and 15.0 GHz, were observed much less frequently, basically a few epochs. All the runs were performed after reports of increased activity from Aql X-1 mainly at optical and X-ray wavelengths, and thus generally trace the outburst history of the object. Given the target of opportunity nature of the observations, the array configurations were varying between runs, standard as well as non-standard, and the effective observing time ranged roughly between 5 and 60 min, with the median around 10–20 min.

We detected Aql X-1 at more than 3σ levels on 7 epochs at 8.4 GHz and 4 epochs at 4.9 GHz. In two occasions the detections were quasi-simultaneous at both frequencies. At least in the cases of some outbursts it is likely that the lack of detection in the radio band is partly due to the very short integration times which generated relatively high noise levels. Here we only discuss part of the data.

When detected, the object was unresolved. All the flux densities reported here are determined via uv-plane fitting and the corresponding errors are estimated based on the rms noise of the images and the differences between flux densities measured in the uv-plane using different initial conditions. Two contaminating sources are present in the field of view, ~ 40 and ~ 290 arcsec away from the position of Aql X-1, and affect the quality of the images in compact configurations at lower frequencies (i.e. 4.9 GHz), however this should not significantly influence the flux measurements. Our values are in agreement, within the errors, with those reported by [35, 36].

2.2 X-ray

We used archival Rossi X-ray Timing Explorer (RXTE) Proportional Counter Array (PCA) and High Energy X-ray Transient Experiment (HEXTE) data on Aql X-1 available in NASA's High Energy Astrophysics Science Archive Research Center (HEASARC).

In the case of the PCA detector, the count rates were extracted using the Standard 2 data, with 16 s time resolution (averaged over each observation). The 129 energy channels were divided in four bands: A: 2.0–3.5 keV; B: 3.5–6.0 keV; C: 6.0–9.7 keV; D: 9.7–16.0 keV. The colours and intensity were determined using the definitions: soft colour= B/A, hard colour=D/C, intensity=A+B+C+D. The instrumental background was subtracted using the latest background models.

The conversion from count rate to Crab was done using the value of the Crab rate closest in time and within the same PCA gain epoch. Furthermore, assuming a Crab-like spectrum $1 \text{ Crab} = 1060 \mu\text{Jy}$. To convert to flux we used the fact that according to WebPimms¹, for a hydrogen column density of $0.5 \times 10^{22} \text{ cm}^{-2}$ [8] and power-law index $\Gamma=2.1$ the unabsorbed flux in the 2-10 keV band is $2.4 \times 10^{-8} \text{ erg cm}^{-2} \text{ s}^{-1}$.

Furthermore, we extracted 20–200 keV count rates from the HEXTE, averaged over each observation. For that purpose we used background subtracted data from cluster A (all detectors) and applied dead-time correction.

2.3 Optical

We present part of the data from the long-term monitoring campaign on Aql X-1 reported in [26]. The R-band observations were made using the ANDICAM² instrument on the 1.0 m and 1.3 m Small and Moderate Aperture Research Telescope System (SMARTS) at Cerro Tololo Inter-American Observatory (CTIO).

Around 83 percent of the quiescent R-band flux is estimated to come from the contaminating star [43] and was thus subtracted from the total observed flux from all the observations.

For magnitude to flux conversion it was assumed that R=0 magnitude corresponds to 3064 Jy [3, 2]. In [7] the colour excess of Aql X-1 was estimated as $E(B-V)=0.5 \pm 0.1$. The R-band extinc-

¹<http://heasarc.gsfc.nasa.gov/Tools/w3pimms.html>

²<http://www.astro.yale.edu/smarts/ANDICAM>

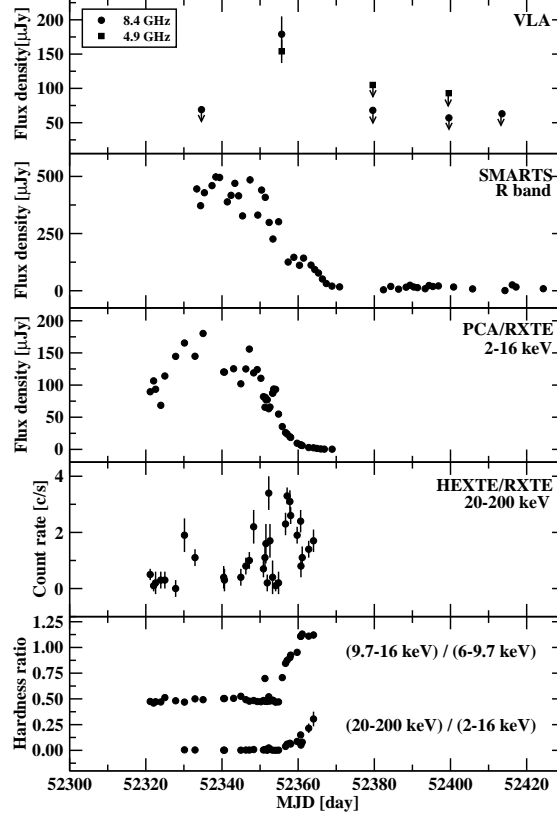


Figure 1: Multiwavelength light curves for the outburst of Aql X-1 from 2002 March and the variation of the hardness ratio between two PCA bands (9.7–16 keV and 6–9.7 keV), and the HEXTE (20–200 keV) and PCA (2–16 keV) bands. If not appearing in the plots, the errors are smaller than the size of the points.

tion A_R was determined using the standard total to selective extinction coefficient $A_V/E(B-V)=3.1$ and the interstellar extinction law $A_R/A_V=0.748$ [34, 4].

3. Multiwavelength light curves

3.1 2002 March outburst

During this outburst (Fig. 1) Aql X-1 was detected in radio quasi-simultaneously at 4.9 and 8.4 GHz and showed then an inverted spectrum (i.e. $F_{8.4} > F_{4.9}$). The optical and PCA data clearly indicate that the source was passing through an active state. It is also apparent that the beginning of the outburst was missed. The level of the HEXTE count rate is low during the ~ 40 days of monitoring and tends to rise slightly towards the end of the data set. As indicated by the hardness ratio, most of the period the system was in a soft state which it left suddenly and transited quickly to a hard state. The radio detections correspond to this X-ray state transition.

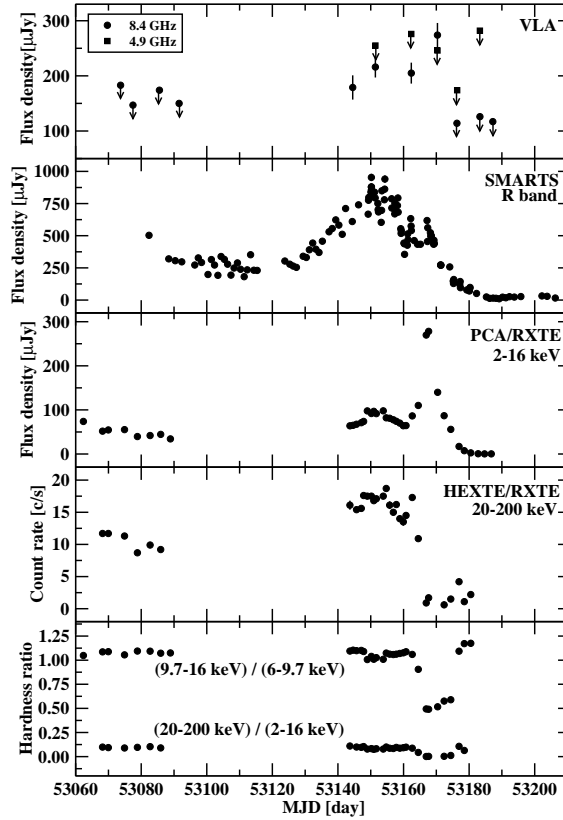


Figure 2: Multiwavelength light curves for the outburst of Aql X-1 from 2004 May–June and the variation of the hardness ratio between two PCA bands (9.7–16 keV and 6–9.7 keV), and the HEXTE (20–200 keV) and PCA (2–16 keV) bands. If not appearing in the plots, the errors are smaller than the size of the points.

3.2 2004 May–June outburst

This is so far, relatively speaking, the most well covered outburst of Aql X-1 in the radio band (Fig. 2). The source was detected on 4 occasions and only at 8.4 GHz, however the lack of detection at 4.9 GHz might be partly attributable to the high rms noise due to the short integration times. On the epoch with the highest 8.6 GHz flux density detected, the contemporaneous upper limit at 4.9 GHz allows to constrain the spectrum in this frequency range to an inverted one. The optical light curve is well sampled and the PCA data reveal a major outburst preceded by a smaller flaring event at about MJD 53150. The HEXTE detector registered a drop in the count rate concomitant with the onset of the flux density increase in the PCA band. This is evident also in the hardness ratio diagram which indicates that during the active period the system made a series of X-ray state transitions, from hard to soft and back to hard. A similar behaviour is observed for the smaller flare, with the difference that in this case the system never reached the soft state, but only temporarily softened its spectrum. The increases in the radio flux density seems to trace the flux density enhancements in the PCA band.

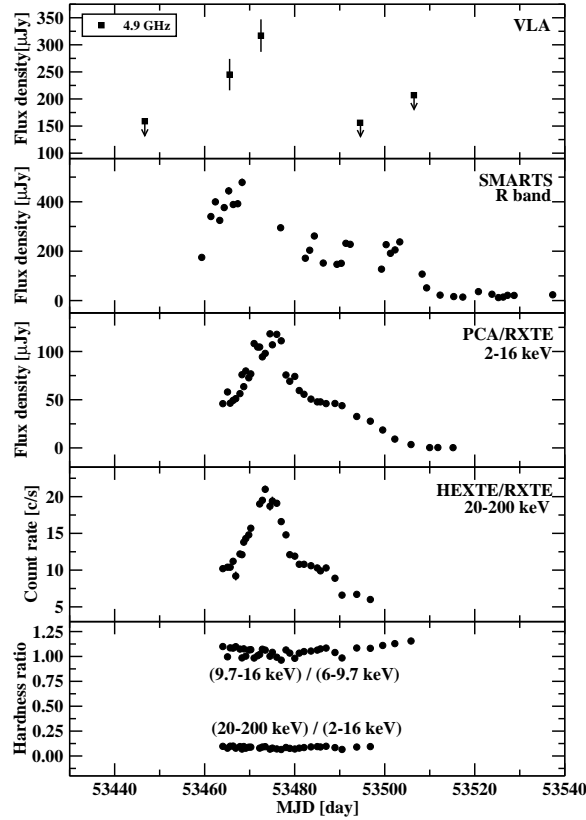


Figure 3: Multiwavelength light curves for the outburst of Aql X-1 from 2005 April and the variation of the hardness ratio between two PCA bands (9.7–16 keV and 6–9.7 keV), and the HEXTE (20–200 keV) and PCA (2–16 keV) bands. If not appearing in the plots, the errors are smaller than the size of the points.

3.3 2005 April outburst

For this outburst (Fig. 3), observations at 8.4 GHz were not available. Aql X-1 was detected twice at 4.9 GHz. The optical data is quite sparse and the outset of the burst was not covered well. The PCA and HEXTE flux density peaks are more or less coincident. The hardness ratio diagram reveals that the system never left the hard X-ray state during the active period.

4. Hardness–Intensity diagrams

The hardness-intensity diagrams (HIDs) corresponding to the three outbursts are represented in Fig. 4. The hardness was determined using the ratio of the PCA bands 9.7–16.0 and 6.0–9.7 keV. The flux density covers the 2.0–16.0 keV energy range. Note that the scales for all the HIDs are identical. The system is tracing the HIDs counter-clockwise.

In 2002 March (Fig. 4, upper-left) the radio upper-limit denoted “A” corresponds to a soft X-ray state of the system at a relatively high X-ray flux density. This situation is reminiscent of the

similar behaviour observed in BHXRBS, when the radio emission is quenched above some X-ray flux density level. The system stays in a soft X-ray state for a while and then makes a fast transition to a hard state. The radio detection (“B”) caught the system during this transitional phase.

In 2004 May–June (Fig. 4, bottom-left) the system traced a full cycle in the diagram. It looks strikingly similar to the “turtle head” HIDs observed in BHXRBS (e.g. [14]) and recently in a dwarf nova [22]. The first four radio non-detections (“A” to “D”) as well as the first three detections (“E” to “G”) correspond to a hard X-ray state. Then suddenly the system jumped to a soft X-ray state and the radio flux density increased significantly (“H”). On a timescale analog to the rise of the radio flux density, the system went below the radio detection limit, back to a hard X-ray state (“I”, “J”).

In 2005 April (Fig. 4, upper-right) the system stayed constantly in a hard X-ray state. It experienced what is sometimes called a hard outburst (e.g. [30]). Whether this can be seen as a failed hard-to-soft outburst, or it is something intimately different it is not clear.

Fig. 4 strongly suggests that a hysteresis phenomenon is at work in Aql X-1. This kind of behaviour was previously noted [25, 24]. In fact, a HID with all the PCA data for all the X-ray outbursts of Aql X-1 between 1997 and 2008 (to be presented elsewhere) clearly shows the “turtle head” as in the bottom-right diagram of Fig. 4.

5. Correlations

Due to space limitations these results will be presented in detail elsewhere. We have extended the work of [30] and studied the radio/X-ray correlation in Aql X-1. We found it to be different than for another atoll source for which a similar amount of data exists, 4U 1728-34. It is not clear yet whether this difference is real or an artifact due to small number statistics. We confirm the results of [26] with respect to the existence of correlations between the optical/soft-X-ray bands by using PCA data instead of ASM as in the previous work. Moreover, we also found correlations between the optical/hard-X-ray bands using HEXTE data. Interesting enough, these correlations are different for hard and soft X-ray states.

6. Conclusions

The light curves of Aql X-1 show quite a rich variety of behaviour during the outbursts. Despite this, the outbursts seem to follow a strict general trend as revealed by the HIDs. The similarity with the BXHRBS and dwarf novae HIDs suggests that the accretion/ejection process works in an analogous way for all these classes of objects. The existence of correlations in the radio/optical/X-ray bands and their dependence on the X-ray state of the system is evidence for two distinct modes of the disc/jet coupling, perhaps related to the size of the accretion disc.

Acknowledgments

The National Radio Astronomy Observatory is a facility of the National Science Foundation operated under cooperative agreement by Associated Universities, Inc..

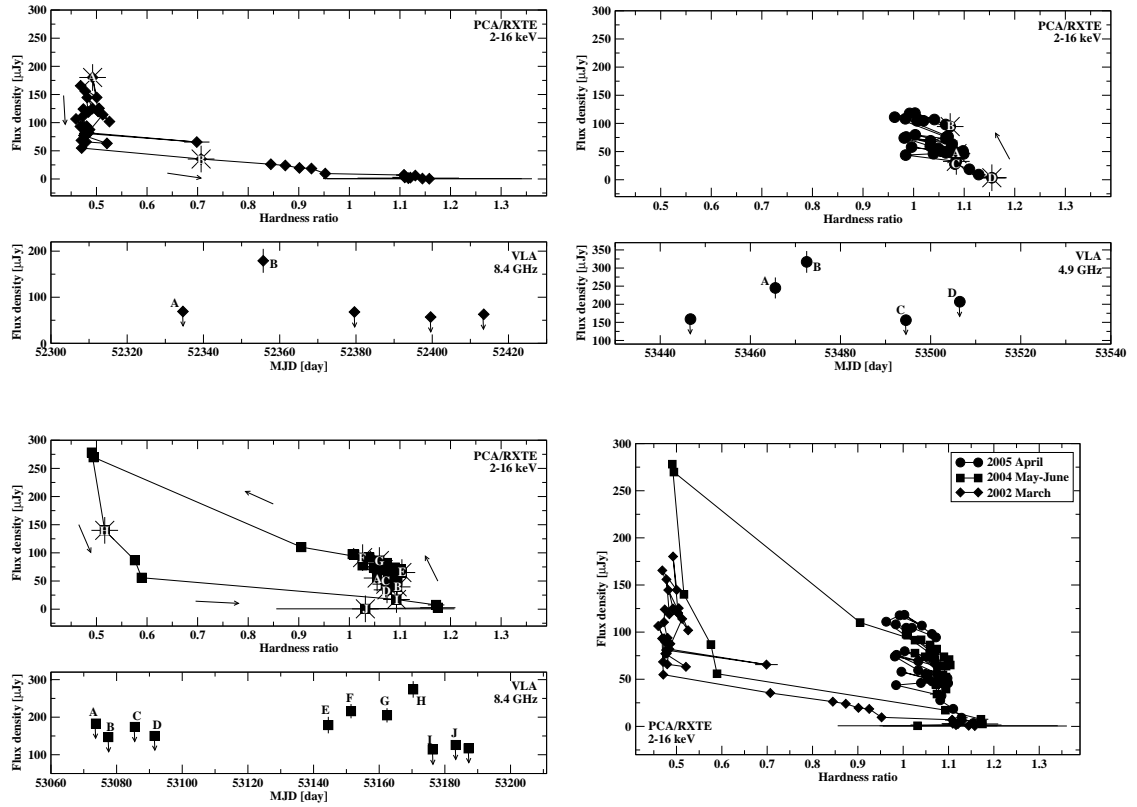


Figure 4: HIDs for the outbursts of Aql X-1 from 2002 March (upper-left), 2004 May–June (bottom-left) and 2005 April (upper-right). The cumulative HID for the all three outbursts is represented in the bottom-right.

References

- [1] Barret D., Boutelier M., Miller M.C., 2008, MNRAS, 384, 1519
- [2] Bessell M.S., Castelli F., Plez B., 1998, A&A, 333, 231
- [3] Campins H., Rieke G.H., Lebofsky M.J., 1985, AJ, 90, 896
- [4] Cardelli J.A., Clayton G.C., Mathis J.S., 1989, ApJ, 345, 245
- [5] Casella P., Altamirano D., Patruno A., Wijnands R., van der Klis M., 2008, ApJ, 674, L41
- [6] Chevalier C., Ilovaisky S.A., 1991, A&A, 251, L11
- [7] Chevalier C., Ilovaisky S.A., Leisy P., Patat F., 1999, A&A, 347, L51
- [8] Church M.J., Balucińska-Church M., 2001, A&A, 369, 915
- [9] Corbel S., Nowak M.A., Fender R.P., Tzioumis A.K., Markoff S., 2003, A&A, 400, 1007
- [10] Corbel S., Körding E., Kaaret P., 2008, accepted in MNRAS, arXiv:0806.3079
- [11] Cui W., Barret D., Zhang S.N., Chen W., Boirin L., Swank J., 1998, ApJ, 502, L49
- [12] Dickey J.M., Lockman F.J., 1990, ARA&A, 28, 215

- [13] Fender R.P., Kuulkers E., 2001, *MNRAS*, 324, 923
- [14] Fender R.P., Belloni T.M., Gallo E., 2004, *MNRAS*, 355, 1105
- [15] Fender R.P., 2006, in *Cambridge Astrophysics Series*, No. 39, *Compact Stellar X-ray Sources*, eds. W. Lewin & M. van der Klis, p. 381
- [16] Gallo E., Fender R.P., Pooley G.G., 2003, *MNRAS*, 344, 60
- [17] Gallo E., Fender R.P., Miller-Jones J.C.A., Merloni A., Jonker P.G., Heinz S., Maccarone T.J., van der Klis M., 2006, *MNRAS*, 370, 1351
- [18] Garcia M.R., Callanan P.J., McCarthy J., Eriksen K., Hjellming R.M., 1999, *ApJ*, 518, 422
- [19] Hasinger G., van der Klis M., 1989, *A&A*, 225, 79
- [20] Hjellming R.M., Han X., 1995, in *X-ray Binaries*, eds. W.H. Lewin, J. van Paradijs, E.P.J. van den Heuvel, p. 308
- [21] Jonker P.G., Nelemans G., 2004, *MNRAS*, 354, 355
- [22] Körding E.G., Rupen M., Knigge C., Fender R., Dhawan V., Templeton M., Muxlow T., 2008, *Science*, 320, 1318
- [23] Koyama K., Inoue H., Makishima K., Matsuoka M., Murakami T., Oda M., Osgawara Y., Ohashi T., Shibasaki N., Tanaka Y., Marshall F.J., Kondo I.S., Hayakawa S., Kunieda H., Makino F., Masai K., Nagase F., Tawara Y., Miyamoto S., Tsunemi H., Yamashita K., 1981, *ApJ*, 247, L27
- [24] Maccarone T.J., Coppi P.S., 2003, *MNRAS*, 338, 189
- [25] Maitra D., Bailyn C.D., 2004, *ApJ*, 608, 444
- [26] Maitra D., Bailyn C.D., 2008, accepted in *ApJ*, arXiv:0807.3542
- [27] Martí J., Mirabel I.F., Rodriguez L.F., Chaty S., 1998, *A&A*, 332, L45
- [28] Migliari S., Fender R.P., Rupen M., Jonker P.G., Klein-Wolt M., Hjellming R.M., van der Klis M., 2003, *MNRAS*, 342, L67
- [29] Migliari S., Fender R.P., Rupen M., Wachter S., Jonker P.G., Homan J., van der Klis M., 2004, *MNRAS*, 351, 186
- [30] Migliari S., Fender R.P., 2006, *MNRAS*, 366, 79
- [31] Moore C.B., Rutledge R.E., Fox D.W., Guerriero R.A., Lewin W.H.G., Fender R., van Paradijs J., 2000, *ApJ*, 532, 1181
- [32] Prins S., van der Klis M., 1997, *A&A*, 319, 498
- [33] Reig P., Méndez M., van der Klis M., Ford E.C., 2000, *ApJ*, 530, 916
- [34] Rieke G.H., Lebofsky M.J., 1985, *ApJ*, 288, 618
- [35] Rupen M.P., Mioduszewski A.J., Dhawan V., 2004, *ATel*, 286, 1
- [36] Rupen M.P., Mioduszewski A.J., Dhawan V., 2005, *ATel*, 491, 1
- [37] Rutledge R.E., Bildsten L., Brown E.F., Pavlov G.G., Zavlin V.E., 2001, *ApJ*, 559, 1054
- [38] Schoelkopf R.J., Kelley R.L., 1991, *ApJ*, 375, 696
- [39] Shahbaz T., Casares J., Charles P.A., 1997, *A&A*, 326, L5
- [40] Šimon V., 2002, *A&A*, 381, 151

- [41] van der Klis M., 1989, ARA&A, 27, 517
- [42] van der Klis M., 1994, ApJS, 92, 511
- [43] Welsh W.F., Robinson E.L., Young P., 2000, AJ, 120, 943
- [44] Xue Y.Q., Cui W., 2007, A&A, 466, 1053